Journal Pre-proof

The role of efflorescent salts associated with sulfide-rich mine wastes in the short-term cycling of arsenic: Insights from XRD, XAS, and μ-XRF studies

N.E. Nieva, M.G. Garcia, L. Borgnino, L.G. Borda

PII: S0304-3894(20)32148-8

DOI: https://doi.org/10.1016/j.jhazmat.2020.124158

Reference: HAZMAT124158

To appear in: *Journal of Hazardous Materials*

Received date: 5 June 2020
Revised date: 2 September 2020
Accepted date: 29 September 2020

Please cite this article as: N.E. Nieva, M.G. Garcia, L. Borgnino and L.G. Borda, The role of efflorescent salts associated with sulfide-rich mine wastes in the short-term cycling of arsenic: Insights from XRD, XAS, and μ-XRF studies, *Journal of Hazardous Materials,* (2020) doi:https://doi.org/10.1016/j.jhazmat.2020.124158

This is a PDF file of an article that has undergone enhancements after acceptance, such as the addition of a cover page and metadata, and formatting for readability, but it is not yet the definitive version of record. This version will undergo additional copyediting, typesetting and review before it is published in its final form, but we are providing this version to give early visibility of the article. Please note that, during the production process, errors may be discovered which could affect the content, and all legal disclaimers that apply to the journal pertain.

© 2020 Published by Elsevier.

The role of efflorescent salts associated with sulfide-rich mine wastes in the short-term cycling of arsenic: insights from XRD, XAS, and μ-XRF studies

N. E. Nieva[a,b], M. G. Garcia[a,c*], L. Borgnino[a,c], L. G. Borda[a]

[a] *Centro de Investigaciones en Ciencias de la Tierra (CICTERRA), CONICET -UNC, Argentina.*

[b] *FTCA Universidad Nacional de Catamarca*

[c] *FCEFyN Universidad Nacional de Córdoba, Córdoba, Argentina*

*Corresponding author at: Av. Vélez Sarsfield 1611, X5016GCA Córdoba, Argentina.
E-mail address: gabriela.garcia@unc.edu.ar

Abstract

The evaporation of As-rich leachates generated by the weathering of sulfide-rich mine wastes accumulated in abandoned tailing dams of the La Concordia mine, triggers the widespread precipitation of saline crusts and efflorescences. Because these salts are highly soluble, they may release high concentrations of arsenic after rainfall events. Thus, the goal of this work is to assess the solid speciation of As in these efflorescences, which may help to understand the short-term cycling of As in the site. The results reveal that As is present only as As(V), while its capacity to be retained in the salts highly depends on their mineralogical composition. Hydrous sulfates, such as gypsum and epsomite show a very low capacity to scavenge As, while copiapite retains the highest concentrations of this element. The spectroscopic evidences suggest that in this mineral, As(V) is included within the lattice, substituting sulfate in the tetrahedral sites. Because copiapite is highly soluble, it may be considered as one of the most important transient reservoirs of As in the site that can release high concentrations of this hazardous pollutant during the occasional rainfall events produced during the wet season.

Keywords*: salt efflorescences- copiapite - AMD - XAS*

Journal Pre-proof

1. Introduction

Acid mine drainage (AMD) is a common product of the alteration of metal sulfide wastes in areas where abandoned or still active metal sulfide mining operations are present. Leakage of this highly acidic solution, rich in toxic metals and metalloids may negatively affect the quality of water in nearby reservoirs. In recent years however, the studies of the solid products of the alteration of metal sulfide wastes are gaining attention, because these materials can scavenge the metals released by sulfide alteration upon exposure to the atmospheric agents. The newly-formed minerals, that usually precipitate by the evaporation of the acid drainage in the form of saline efflorescences or spread within the residues, mainly consist of efflorescent (hydrated) sulfates, Fe(III) (oxy)hydroxides, (oxy)hydroxysulfates, (sulfo)arsenates, and (sulfo)arsenites (e.g., Drahota and Filippi, 2009; Lottermoser, 2010; Majzlan et al., 2014). Due to the high solubility of many of these efflorescent minerals, the climate has an important control over their formation and the consequent mobilization or retention of metals and metalloids. In arid and semiarid climates with prolonged dry periods, thick crusts of salts usually form at the mine site by evaporation of the effluents resulting of the sulfide alteration, that migrate upward by capillary action (Olyphant et al., 1991; Dold, 1999). Because these salts are highly soluble, they represent a temporal source of pollution to the water, as they release metals and metalloids after rainfall events. The cycle of salt precipitation and dissolution results in seasonal variations in water quality, that adversely affect surrounding ecosystems (Alpers et al., 1994).

Arsenic (As) is one of the most hazardous contaminants released by the oxidation of sulfide-rich mine wastes, due to its toxicity and high mobility in natural environments. In arid regions impacted by acid drainage, As may co-precipitate as an impurity along with a wide variety of secondary minerals, such as schwertmannite and

jarosite (e.g., Nordstrom and Alpers, 1999; Bigham and Nordstrom, 2000) as well as metal arsenates and sulfoarsenates (Drahota and Filippi, 2009). These secondary phases may precipitate either as amorphous, poorly crystalline or well-crystallized products, cementing and encrusting tailings particles on a laterally extensive or discontinuous scale (Lottermoser and Ashley, 2006). A number of works have reported the preferential association of As with amorphous or poorly crystalline ferric (hydr)oxides, as well as with reactive ferric arsenates formed as alteration products of primary sulfides. Most of them proposed that the desorption from these minerals or even their dissolution control the release of As to the water (e.g., Drahota et al., 2016; Nieva et al., 2016; Kocourková et al., 2011; Lottermoser, 2010).

The abandoned Concordia mine waste dump (Fig. 1; 4200 m a.s.l.) represents a local source of As pollution in the Puna region of Argentina (Central Andes). In this region, climate is semiarid, characterized by wide daily temperature variations and rainfall concentrated in one season. The annual average precipitation during the fall-winter seasons is 30 mm, and 149 mm in spring and summer (Bianchi y Yánez, 1992). The mean annual temperature in the area is 8.7°C, but temperatures as high as 40°C can be recorded during summer while in winter night temperatures of about -25°C are frequent. The region has a negative water balance throughout the year; evapotranspiration is maximum in the summer months (exceeds 900 mm $year^{-1}$) coinciding with the summer precipitation regime.

Journal Pre-proof

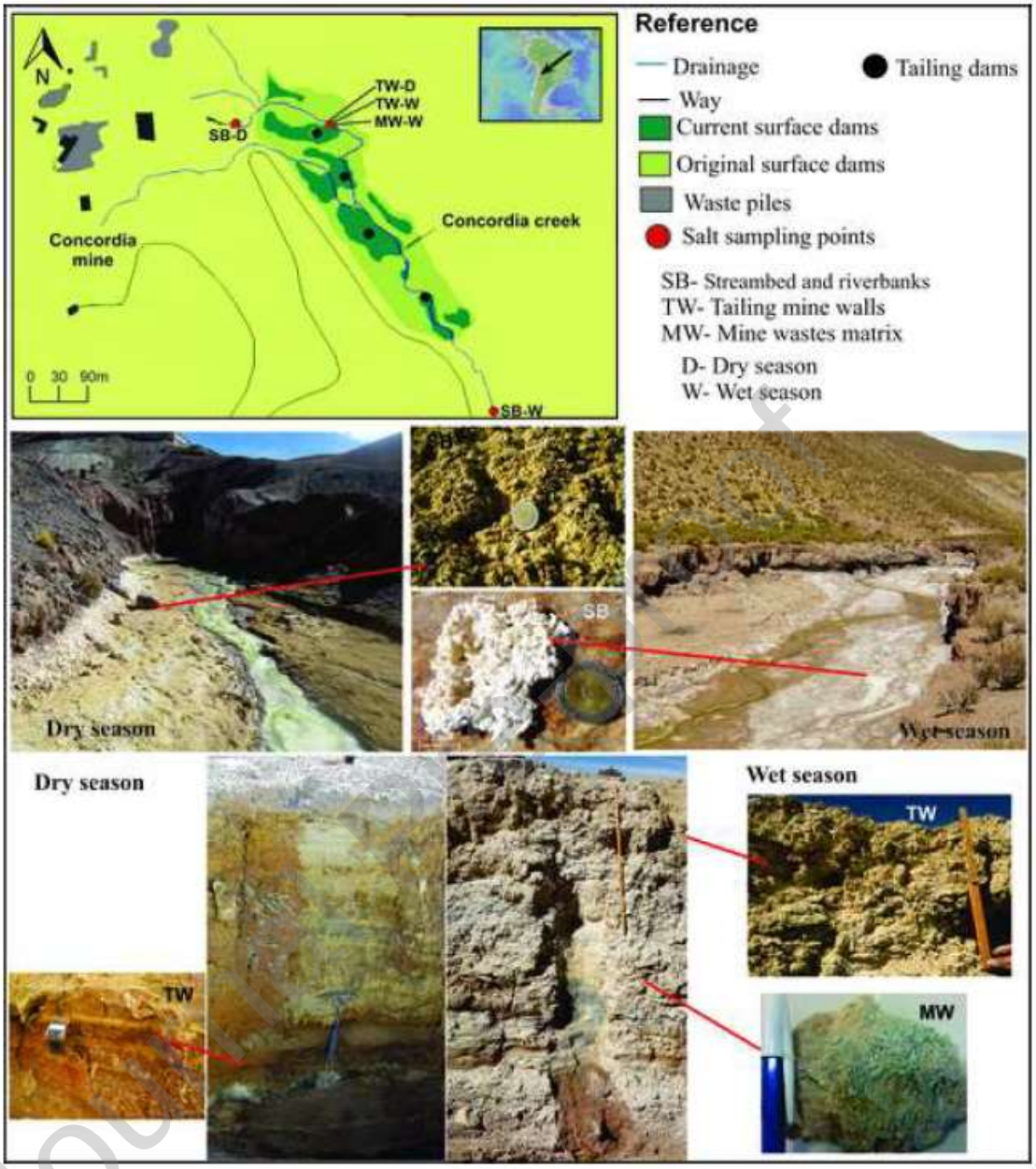

FIGURE 1. Map of La Concordia mine site showing the location of the sampling points. The images show the characteristics of the salts crusts formed at the Concordia´s streambed and at the tailing sidewalls ans pores in the two sampling periods.

The Concordia mine exploited Pb, Ag, and Zn from an epithermal ore deposit of high sulfidation type (Zappettini, 1990), until 1986 when the activities finished (Argañaraz et al., 1982). In operation, the residues were stored in four tailing dams that were abandoned after closure. In the following 30 years, the oxidation of metal sulfides

accumulated in the tailing dams upon weathering agents resulted in the formation of a large variety of secondary minerals and the generation of highly acidic solutions rich in dissolved metals and metalloids that drained into the Concordia creek (Nieva et al., 2016, 2018, 2019). Leaching experiments performed with suspensions of the tailing residues in milliQ water (equilibrium pH ~3) demonstrated that As was rapidly released after 1 h of sediment-water interaction (i.e., Nieva et al., 2016). This fraction was associated with the abundant and highly soluble metal hydrated sulfates identified by SEM/EDS and XRD measurements in the salts spread on the mine site surface. XAS analysis performed in these wastes (i.e., Nieva et al., 2019) revealed that the more labile As-phases correspond to amorphous ferric arsenates and arsenate ions adsorbed on or included into jarosite/schwertmannite. Despite the leaching of the mine wastes can contribute high concentrations of As and heavy metals to the Concordia Creek (Nieva et al., 2016; 2018), it has been demonstrated that sulfate salts associated with mine wastes are also a hazardous source of periodic contamination, particularly after rainfall events (e.g., Bayless and Olyphant, 1993; Alpers et al., 2000; Frau, 2000; Jerz and Rimstidt, 2003; Cánovas et al., 2008, 2010). Regarding the high concentrations of As determined in saline crusts deposited at the Concordia mine site (i.e., Nieva et al., 2016), it is expected that their dissolution due to flush out processes at the beginning of the spring rainfalls may produce peaks of increasing concentrations of As in the Concordia Creek´s waters. Therefore, the aim of this work is to assess the As solid speciation in saline efflorescences formed by the evaporation of the AMD, which may help to understand the short-term cycling of As in mine-waste disposal sites.

Journal Pre-proof

2. Materials and methods

2.1. Sampling

Samples were collected from three main locations in the mine site: a) streambed and riverbanks; b) exposed walls of the tailing dams, and c) salts disseminated as small crystalline aggregates in the mine wastes (Fig. 1). Samplings were carried out in June 2014, during the dry season, and in April 2016, at the end of the wet season. Samples were collected using a Teflon shovel in order to avoid metal contamination, double bagged in sealed low O_2 diffusion plastic bags and transported to the laboratory refrigerated at 4 °C, where they were air-dried before analysis.

2.2. Mineralogical analysis

The mineral characterization by X-ray powder diffraction (XRPD) was performed using a Philips X'Pert Pro diffractometer (40 kV, 40 mA), in Bragg–Brentano reflection geometry with Cu Kα radiation (λ = 1.5418Å). The data were recorded between 5° and 70° (2θ) in steps of 0.02° and 10 s per step. The refinement of the crystal structures was performed by the Rietveld method (Rietveld., 1969) using the FULLPROF program (Rodríguez-Carvajal, 1993). A pseudo-voigt shape function was adequate to obtain good fits in all cases.

2.3. Chemical analysis

The chemical composition of salts was determined in extracts obtained after dissolution in deionized water (18 MΩ cm^{-1}, MilliQ, Millipore Corp.). About 1.00 g of sample was dissolved in 50 ml of MilliQ water, using polypropylene tubes with plug seal cap, and stirred for 1 day. The obtained leachate (equilibrium pH 3-4), that corresponds to the water soluble fraction of the salts, was separated from the residue and analyzed by ICP-MS (Agilent 7500cx). The remaining residue was dried and weighted in order to calculate the mass of dissolved salts. For elemental determinations, calibration curves

were run before the samples measurements. The calibration solutions were prepared using ultrapure 2% HNO_3, and certified stock solutions. Sample blanks were analyzed every set of 8-10 samples for correction of background effect on instrument response. Metal concentrations in the samples were calculated with the ChemStation spectrometer software. The limits of detection were calculated as three times the instrumental standard deviation, obtained after 10 replicates of blank solutions.

2.4. μX-ray fluorescence (μ-XRF) and μ-XANES analysis

X-ray fluorescence measurements were performed at the D09B XRF beamline of the Laboratório Nacional de Luz Síncrotron (LNLS), in Campinas, Brazil (Pérez et al., 1999). In addition, μXANES analyses were performed in specific areas of the XRF maps where high concentrations of As were identified. The setup for *μ*-XRF experiments and for the collection of the μXANES As K-edge spectra of the samples and references is described in detail in the SI file.

2.5. XAS data collection

XAS (X-ray absorption spectroscopy) spectra were collected at the XAFS 2 beamline of the Laboratório Nacional de Luz Síncrotron (LNLS), in Campinas, Brazil. Details of the line setup for the collection of As K-edge and Fe K-edge spectra in both transmission and fluorescence modes, standards and samples preparation, and the methodology followed for the analysis of the XANES and EXAFS data are described in the SI file.

3. Results

3.1 Mineralogical composition of the salts associated with mine wastes

The mineralogical composition of the studied salts is reported in Table 1, while XRD spectra and Rietveld refinement are shown in the supplementary information (SI)

Journal Pre-proof

file. In general, clastic minerals such as quartz and micas are important constituents in the salts collected in the dry season, because these minerals are preferentially transported during winter by the intense winds of the Puna region (e.g., Gaiero et al., 2013) and deposited in the river valley or attached to the tailings sidewalls. On the other hand, the salts formed at the end of the wet season are dominantly composed of evaporitic minerals. Yellowish salts precipitated in the La Concordia streambed during the dry period are composed of apjohnite, quartz, and nearly similar proportions of halotrichite and epsomite. Gypsum and As-jarosite are minor phases in the sample. At the end of the wet season, the riverbanks ´salts are white, and show a quite different mineralogy, as the main component is the Mg-bearing hydrated sulfate epsomite, which represents nearly 50% of the mineralogical composition. Some other hydrated sulfates identified in this sample are tamarugite, apjohnite, szmikite, goslarite, and gypsum.

Table 1. Mineralogical composition of efflorescent salts from La Concordia Mine

		Streambed and riverbanks (SB)		**Tailing mine walls (TW)**		**Mine wastes matrix (MW)**
Phases (%)		dry season	wet season	dry season	wet season	wet season
Quartz	SiO_2	22		69	5	8
Muscovite	$KAl_2(Si_3Al)O_{10}(OH,F)_2$			16		
Gypsum	$CaSO_4•2H_2O$	2	3	5		
Jarosite	$KFe_3^{+3}(SO_4)_2(OH)_6$			4	6	1
As-jarosite	$PbFe_3^{+3}(AsO_4)(SO_4)(OH)_6$	3		2		
Coquimbite	$Fe^{3+}_2(SO_4)_3•9H_2O$				4	30
Copiapite	$Fe^{2+}Fe^{3+}_4(SO_4)_6(OH)_2•20H_2O$				76	43
Halotrichite	$Fe^{2+}Al_2(SO_4)_4•22H_2O$	15				
Apjohnite	$Mn^{2+}Al_2(SO4)_4•22H_2O$	44	5			
Tamarugite	$NaAl(SO_4)_2•6H_2O$		27			
Epsomite	$MgSO_4•7H_2O$	14	49			
Szmikite	$Mn^{2+}SO_4•H_2O$		15	4		
Chalcanthite	$CuSO_4•5H_2O$					18
Goslarite	$ZnSO_4•7H_2O$		1		9	
$\chi 2$		2,42	5,21	3,24	5,80	3,70

The reddish salts formed at the exposed walls of the tailing dams during the dry season are mostly composed of clastic minerals such as quartz and muscovite, while

hydrated and hydroxy sulfates such as gypsum, szmikite, jarosite and As-jarosite are minor constituents. On the contrary, at the end of the wet season, these salts, dominantly of yellow color, are composed of copiapite, with minor presence of quartz, jarosite, As-jarosite, gypsum, and szmikite.

The aggregates of salts disseminated in the wastes show a clear blue color and their mineralogical composition is dominated by copiapite, coquimbite, and chalcanthite, minerals that represent more than 90% of their total composition. The Cu-bearing hydrated sulfate chalcanthite is likely responsible for the characteristic blue greenish color of these salts. Finally, quartz and jarosite are also present, but in much lower proportion.

3.2 Chemical composition of the water-soluble fraction of efflorescent salts

The chemical composition of the water-soluble salts precipitated during the dry and wet seasons on the streambed and riverbanks (SB), and tailing mine walls (TW) is shown in Table 2. The salt aggregates dispersed in the mine wastes matrix (MW) were only identified in the sampling campaign carried out in the wet season, and thus, only chemical data of this period are available. The percentages of the water soluble fraction in these samples is also reported, along with the pH values of the suspensions recorded after 24 h of salt-water reaction.

Table 2. Chemical composition the water-soluble fraction of the study samples after 24 h of salt-water reaction.

Samples	**pH 24h**	**% soluble fraction**	**Na %**	**Mg**	**Al**	**K**	**Ca**	**Fe**	**Mn**	**Cu mg Kg^{-1}**	**Zn**	**As**	**Pb**
Dry season													
TW	2.98	31.6	0.14	1.62	2.28	0.12	0.68	27.10	1.56	276	634	97	27
SB	3.02	70.4	0.33	0.49	0.84	0.01	0.02	1.30	1.16	11	35	6	14
Wet season													
TW	3.11	87.9	1.62	25.63	14.28	0.94	0.41	47.22	9.49	4976	4443	769	44

SB	4.05	95.5	10.16	27.23	19.11	0.28	0.42	0.10	41.96	114	1123	0.24	0.1
MW	3.04	63.4	0.76	6.53	3.20	0.52	0.24	64.28	4.05	3316	2201	204	23

The water-soluble fraction in the salts precipitated at the tailing dams´ sidewalls during the dry season corresponds to nearly 30% of the bulk sample, while in the remaining samples, this fraction is higher than 60%. The pH values of the suspensions varied from 2.3 to 4.0, and they slightly increased with time in the recorded period.

The major chemical composition of the water-soluble salts precipitated in the site is closely associated with the evaporitic minerals identified in them, which are Fe, Mn, and Mg sulfates, with a minor proportion of Al and Ca sulfates. The ternary diagram of Figure 2 represents the variability of the relative contents of Fe, Mn and Mg in the analyzed samples, and shows that the proportion of these elements vary along the hydrological year, regardless of the site in which the sample is located. In the case of the samples collected from the Concordia´s streambed and from the tailing´s sidewalls, the relative content of Fe is much higher than those of Mg and Mn during the dry season, while during the wet season, the relative content of Mg tends to be more important. Because the salt aggregates spread in the tailings sediments matrix were collected only during the wet season, the seasonal variation of their chemical composition cannot be assessed; however, the relative contents of the three major components Fe, Mg, and Mn in this sample is similar to those determined for the soluble salts precipitated on the tailings sidewalls during the dry season.

Journal Pre-proof

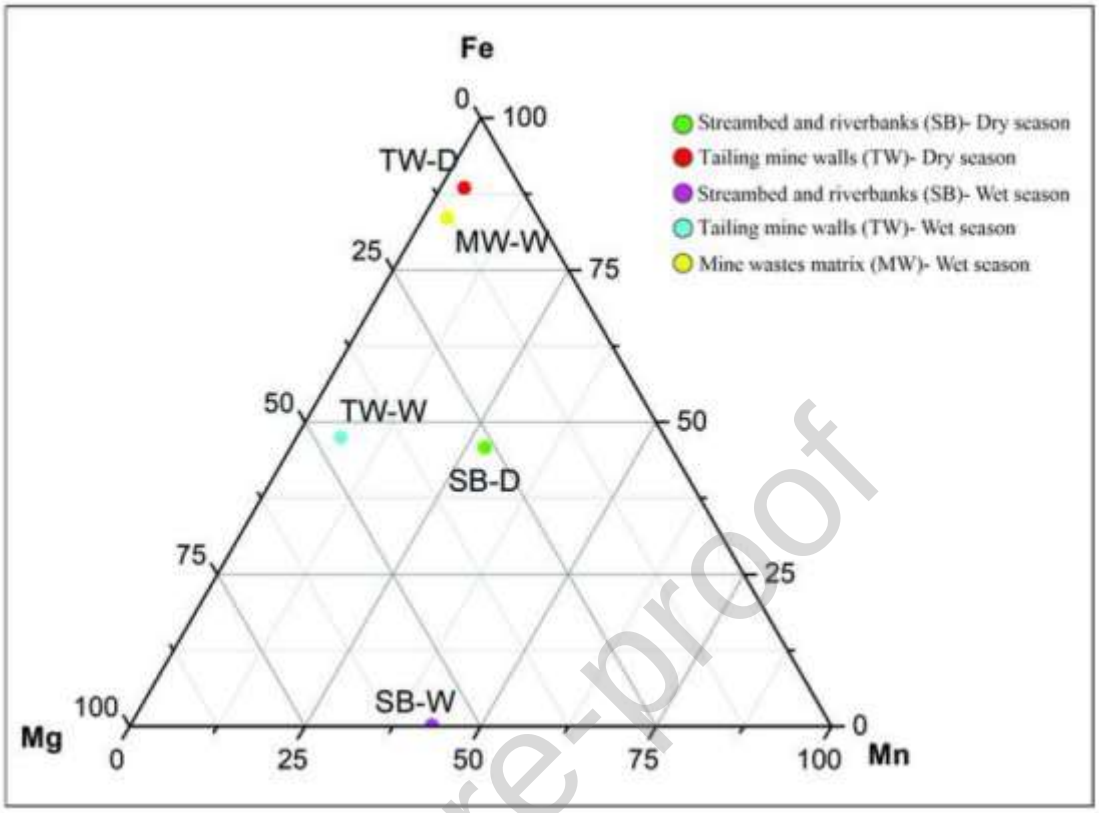

FIGURE 2. Ternary diagram showing the relative contents of Fe, Mn and Mg in the study salt samples.

The As concentrations in the salts precipitated in the site vary from 0.24 to 769 mg Kg^{-1} (Table 2). The highest value was determined in the sample of the yellow salt crust collected from the tailing´s sidewalls at the end of the wet season (sample TW-W), while the lowest correspond to white salts that cover the streambed and riverbanks of the Concordia Creek in the same period (sample SB-W).

4.3 XAS analysis

4.3.1. Fe speciation

Normalized Fe XANES spectra and the corresponding first derivative analysis of samples and reference materials are available in the SI file, as well as the positions of

Journal Pre-proof

the main peaks determined from the first derivative spectra. Because most of the Fe compounds identified in the study samples have overlapping peaks in XANES spectra (O'day et al., 2004), the first derivative values can only be indicative of the oxidation state of Fe.

LCF analysis was conducted in order to quantify the proportion of the Fe phases that were previously identified with the XRD and chemical analyses. The results show that Fe (III) species are dominant in all samples except in the salts precipitated in the tailing matrix and tailing sidewalls during the wet period (Table 3, Fig. 3), where Fe(II) sulfate species represent more than 50% of the total Fe phases in the samples. The Fe(II) species could be assigned to copiapiate, an Fe(II)-Fe(III) mineral that was only identified in these two samples. On the other hand, Fe is present as Fe(III) phases in minerals such as jarosite and copiapite, both of them also identified by XRD, and schwertmannite, a poorly crystalline mineral that is a common product of alteration in sulfide-rich mineral wastes. Besides, a small proportion of Fe(III) in the form of $FeAsO_4$ was fitted in the samples of salts collected from the tailing´s sidewalls.

Table 3. Results of linear combination fits of the Fe K-edge XANES spectra of the Concordia mine salt samples collected during the dry and wet seasons. The energy range in the normalized XANES spectra was 7100–7220 eV. Values in parenthesis correspond to the standard deviation. The residual factor (R) and $\chi 2$ provide a measure of the goodness of the fit.

Samples Salts	**LCF -XANES**				**Statistical parameters**	
	As-Jrs[a]	As-Schw[a]	Scorodite[b]	Ferrous sulfate[c]	χ^2	R *factor*
Dry season						
Streambed and riverbanks (SB)	63.9 (3.5)	32.7 (4.2)		3.5 (5.5)	0.0003	0.0004
Tailing mine walls (TW)	55.2 (2.7)	30.3 (1.8)	11.5 (3.3)	3.1 (0.3)	0.0001	0.0001
Wet season						
Streambed and riverbanks (SB)	65.2 (2.9)	30.9 (3.5)		3.9 (4.6)	0.0002	0.0003
Tailing mine walls (TW)	25.7 (5.9)	21.2 (4.1)	2.3 (0.8)	50.8 (7.3)	0.0003	0.0004
Mine wastes matrix (MW)	3.0 (2.7)	32.9 (3.6)		64.1 (4.5)	0.0002	0.0002

a Synthetic As(V)-jarosite and schwertmannite (Nieva et al., 2019).

b Natural scorodite ($FeAsO_4$).

c Analytical grade reagents ferrous sulfate.

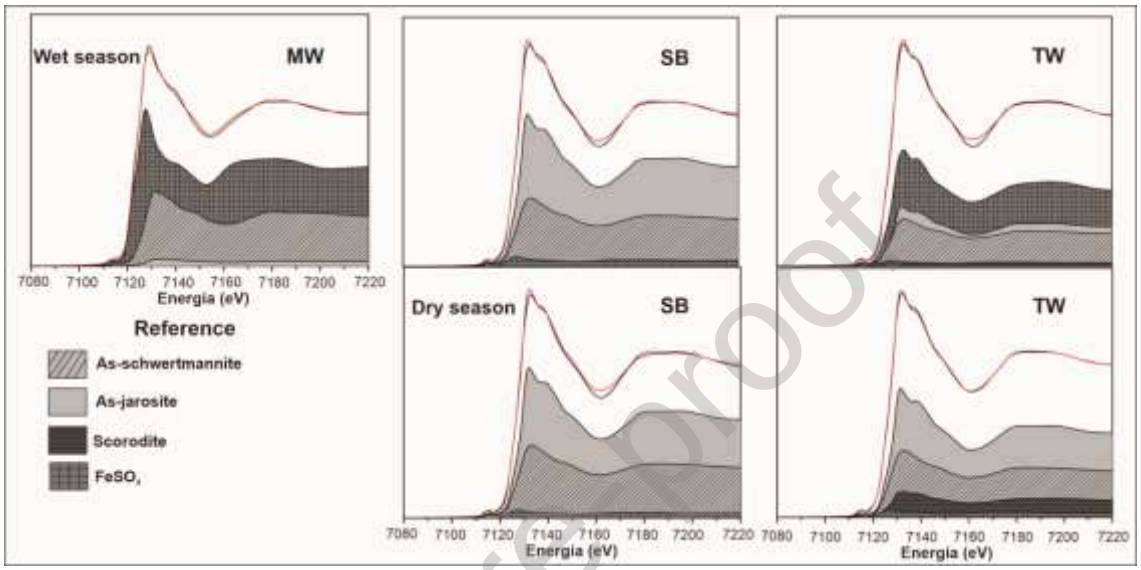

FIGURE 3. Linear combination fits of the Fe K-edge spectra for the study samples. Thick solid lines depict measured spectra; red solid lines indicate fit results. The quantitative data for the fittings are provided in Table 3. All the reference compounds mentioned in the SI file have been considered in the LCF analysis

The analysis of the EXAFS region of the XAS spectra was only performed in samples collected at the tailing´s sidewalls, because only these spectra showed less noisy signals. The Fe-EXAFS parameters fitted in the spectra of the red salts precipitated at the tailing´s walls during the dry season suggest the presence of As-jarosite and schwertmannite. The first shell represents Fe(III) atoms in octahedral coordination with six oxygen atoms (Table 4). The O atoms are positioned in two layers, four of them at 1.95 Å and the remaining two at 2.04 Å. In addition, two S atom are located at 3.24 Å from the central Fe atom. Although these arrangements are typical of jarosite (Menchetti and Sabelli, 1976), the Fe-K shell characteristic of this mineral could not be identified, probably because this signal is depleted due to the

presence of arsenate, as reported by Savage et al. (2005). Besides, the high σ^2 value obtained for the Fe-S shell (σ^2=12.10^{-3} Å^2) indicates that the sulfate tetrahedral site is quite disordered at the short-range scale. Furthermore, an Fe-As shell could be considered in the model, regarding the values of *R* (~3.31 Å) and *N* (3.82). This shell is typical of scorodite (Kitahama et al., 1975), a mineral that was not identified in this sample. Thus, these results could be interpreted as the Fe-As distance in jarosite when sulfate ions are substituted by arsenate (i.e., Savage et al., 2005). In summary, the spectroscopic evidences such as the presence of fourfold-coordinated As with Fe atoms, the absence of the Fe-K shell and the identification of a disordered tetrahedral site clearly suggest the presence of As-substituted jarosite (As-jarosite). Similar arrangements were identified in the Fe-EXAFS spectra of the sediments sampled from the oxidation profiles of the study mine wastes (i.e., Nieva et al., 2019).

Two additional Fe-Fe shells were also fitted, with $R_{Fe\text{-}Fe}$ = ~3.01 and 3.42 Å, and $N_{Fe\text{-}Fe}$ = 1.34 and 3.8 respectively, which are typical values reported for schwertmannite (Maillot et al., 2013; Nieva et al, 2019).

Table 4. EXAFS fitting results at the Fe K-edge for the sample TW-D and TW-W. Experimental and calculated curves are shown in the SI file. Fitted parameters include: *N*, coordination number, *R* (Å), interatomic distance, σ^2 (Å^2), squared Debye-Waller factor, ΔE_0 (eV), energy difference accounting for phase shift between overall experimental spectrum and FEFF calculation.

Sample	Shell	N	R (Å)	σ^2(1x10^{-3} Å^2)	ΔE_0 (eV)	R-*factor*
Dry season						
TW-D	Fe-O	3. 98	1.94	5	6.9	0.001
	Fe-O	2.55	2.04	0.6		
	Fe-S	1.7(*f*)	3.24	12		
	Fe-As	3.82	3.31	8		
	Fe-Fe	1.34	3.01	2		
	Fe-Fe	3.80	3.42	28		
Wet season						
TW-W	Fe-O	3.99	1.94	3	7.6	0.001
	Fe-O	1.82	2.06	2		
	Fe-S	2.12	3.31	6		
	Fe-As	1.89	3.36	0.4		
	Fe-Fe	2(*f*)	3.05	4		
	Fe-Fe	2(*f*)	3.30	21		
	Fe-Fe	1(*f*)	3.63	6		

(f) Fixed parameter.
Standard deviations of *N* (± 0.3 atom), *R* (± 0.3 Å) and ΔE (± 0.2 eV).

Fit quality was estimated using R-*factor*.

In the XAS spectra corresponding to the salts collected at the end of the wet season from the tailing sidewalls, the first shell of coordination corresponds to Fe atoms in octahedral coordination with four O atoms at a distance of 1.94 Å and two apical O atoms at 2.06 Å. The second shell is assigned to Fe-S, characterized by R = 3.31 Å and N= 2.12 (Table 4), while a Fe-As shell, characterized by $R_{Fe\text{-}As}$ = 3.36 Å and N = 1.86 was also fitted. The parameters of the second shell (Table 4) are similar to those reported by Paktunc et al. (2013) for Fe-S in arsenate-bearing Fe(III) sulfates that incorporate increasing concentrations of arsenate in their lattices. Low N values (i.e., ~2) determined for this shell in the study samples might be interpreted as an evidence of arsenate by sulfate substitution in the corresponding sulfate tetrahedral site. The third Fe-Fe shell was fitted by fixing the coordination value (i.e., N =1). The calculated distance (R = 3.63 Å) is assigned to corner linked FeO_6 octahedra along the octahedral chains in arsenate-bearing Fe(III) sulfates. Finally, the distances fitted at 3.05 and 3.3 Å with N = 2 are assigned to Fe-Fe shells in schwertmannite (Forsyth et al., 1968, Maillot et al., 2013).

4.3.2. As speciation

Normalized As XANES spectra and the corresponding first derivative analysis of samples and reference materials are available in the SI file, as well as the positions of the main peaks determined from the first derivative spectra. All samples show edge features corresponding to As(V) compounds, regardless their location in the site and the hydrological condition at the moment of sampling.

According to the LCF results, in all samples collected during the dry season, arsenic is present in the form of three species: 1) As-jarosite; 2) As-schwertmannite,

and 3) Fe arsenates (Figure 4). At the end of the wet season, only species 1) and 2) were identified in the study salts (Table 5).

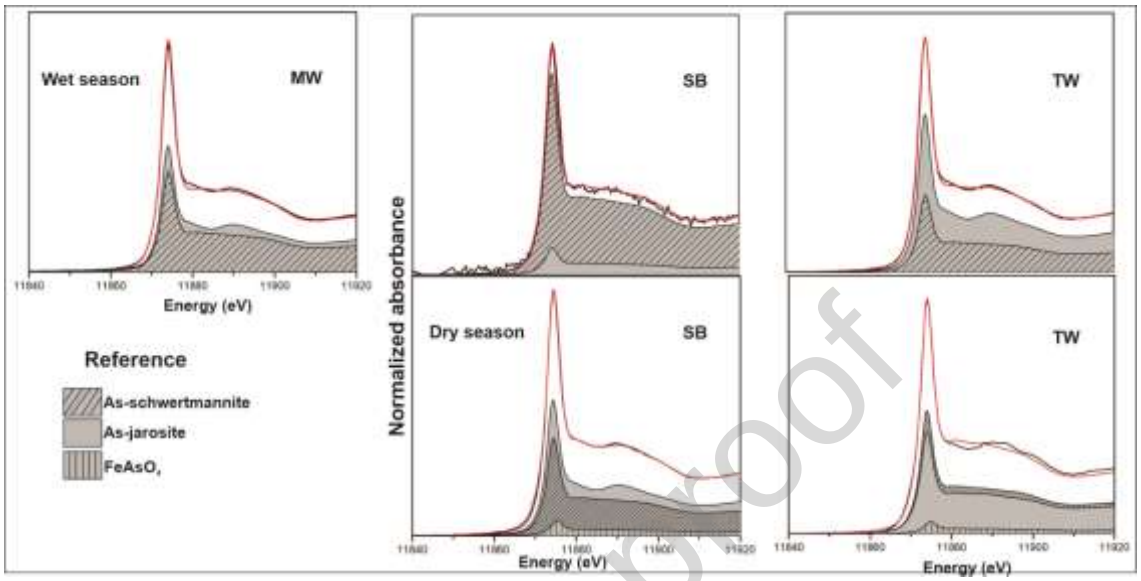

FIGURE 4 Linear combination fits of the As K-edge spectra for the study samples. Thick solid lines depict measured spectra; red solid lines indicate fit results. The quantitative data for the fittings are provided in Table 5. All the reference compounds mentioned in the SI file have been considered in the LCF analysis

Table 5. Results of linear combination fits performed on As K-edge XANES data of saline samples. Linear combinations were made with the Athenas program (Ravel and Newville, 2005). The energy range in the normalized XANES spectra was 11,840–11,920 eV. The residual factor (R) and $\chi 2$ provide a measure of the goodness of the fit.

Samples		LCF - XANES		Statistical parameters	
	As(V)-Jrs [a]	As(V)-Schw [a]	Scorodite[b]	X^2	R *factor*
		Dry season			
Streambed and riverbanks (SB)	52.7 (0.4)	40.7 (0.5)	6.6 (0.7)	0.0005	0.0005
Tailing mine walls (TW)	44.2 (1.4)	50.5 (1.0)	5.3 (1.7)	0.0016	0.0020
		Wet season			
Streambed and riverbanks (SB)	11.9 (9.9)	88.1 (9.6)		0.0031	0.0037
Tailing mine walls (TW)	66.3 (0.4)	33.7 (0.4)		0.0005	0.0004
Mine wastes matrix (MW)	56.3 (0.6)	43.7 (0.7)		0.0010	0.0008

Values in parenthesis correspond to the standard deviation.

[a] Synthetic As(V)-Jrs and Schw (Nieva et al., 2019)

[b] Natural Scorodite ($FeAsO_4$).

Like in the case of Fe, the EXAFS region of the As K-edge spectra could only be analyzed in the samples collected from the tailing´s sidewalls in both seasons. In the sample collected during the dry season, the first shell corresponds to arsenate compounds in a tetrahedral structure, with oxygen atoms located at 1.68 Å from the central atom (Table 6). This group may correspond to either arsenate ions sorbed onto mineral surfaces or included within mineral's lattices. The second As-Fe shell is characterized by *R* = 3.25 Å and *N*= 2.2 (Table 6), values that have been already reported for arsenate groups included within the jarosite lattice (i.e., Paktunc and Dutrizac, 2003; Savage et al., 2005; Nieva et al., 2019).

Table 6. EXAFS fitting results at the As K-edge of the studied samples. Experimental and calculated curves are shown in the SI file. Fitted parameters include: *N*, coordination number, *R* (Å), interatomic distance, σ^2 ($Å^2$), squared Debye-Waller factor and ΔE_0 (eV), energy difference accounting for phase shift between overall experimental spectrum and FEFF calculation.

Samples	Shell	N	R (Å)	σ^2($1x10^{-3}$ $Å^{2)}$	ΔE_0 (eV)	R-*factor*
Dry season						
TW-D	As-O	3.92	1.68	2	0.25	0.002
	As-Fe	2.22	3.25	9		
Wet season						
TW-W	As-O	3.97	1.68	1	7.48	0.007
	As-Fe	4.20	3.34	5		
	As-Fe	2.80	3.53	2		

Standard deviations of *N* (± 0.4 atom), *R* (± 0.1 Å) and ΔE (± 0.5 eV).
Fit quality was estimated using R-*factor*.

In the sample collected during the wet season (TW-W), the first shell of coordination also corresponds to arsenate groups. The parameters of the second shell are similar to those reported for arsenate-bearing Fe(III) sulfates ($R_{Fe\text{-}As}$ = 3.34 Å and *N*=4.2; Paktunc et al., 2013). These results are in agreement with the results of the Fe-EXAFS analysis (i.e., Fe-As shell) that revealed arsenate by sulfate substitution in

arsenate-bearing Fe(III) sulfates (Paktunc et al., 2013). Finally, the As-Fe shell fitted at longer distances (i.e., *R* = 3.53 Å), likely corresponds to adsorbed arsenate monodentate complexes, which typically show interatomic distances at 3.6 Å (Waychunas et al., 1995).

4.4 Elemental associations (μ-XRF mapping) and identification of As speciation (μ-XANES) in selected mineral grains

The spatial distribution of elements at a micrometric scale was analyzed in specific mineral grains of salts collected during the dry period by μ-XRF mapping. This technique allows obtaining distribution maps of elements such as S, Fe, As, Ca, and K at a precision of 0.5 μm.

Figure 5 shows the elemental maps obtained for some individual grains present in the sample collected from the tailings 'walls during the dry season. In this sample, three zones of different composition can be identified: (i) areas rich in Ca and S that correspond to grains of gypsum, in which As was not detected (Fig. 5a, spots 1); (ii) areas rich in Fe, S and K that correspond to jarosite grains (Fig. 5b, spot 2); and (iii) areas rich in Fe and S (without K) that likely correspond to schwertmannite (Fig. 5c, spot 3). The areas enriched in As (Fig. 5c, spot 4) are mostly located at the edges of the jarosite and schwertmannite grains which explains the good correlation between the contents of As and Fe in the sample (Fig. 5 d). The As K-edge μ-XANES measurements performed in these zones, produced a peak at 11,873 eV, indicating the presence of As (V) species (data available in the SI file). LCF analysis suggests that the main As-bearing phases present in the analyzed grains correspond to arsenate ions included in jarosite and in lesser extent to an Fe arsenate compound (Figure 5e, Table 5).

Journal Pre-proof

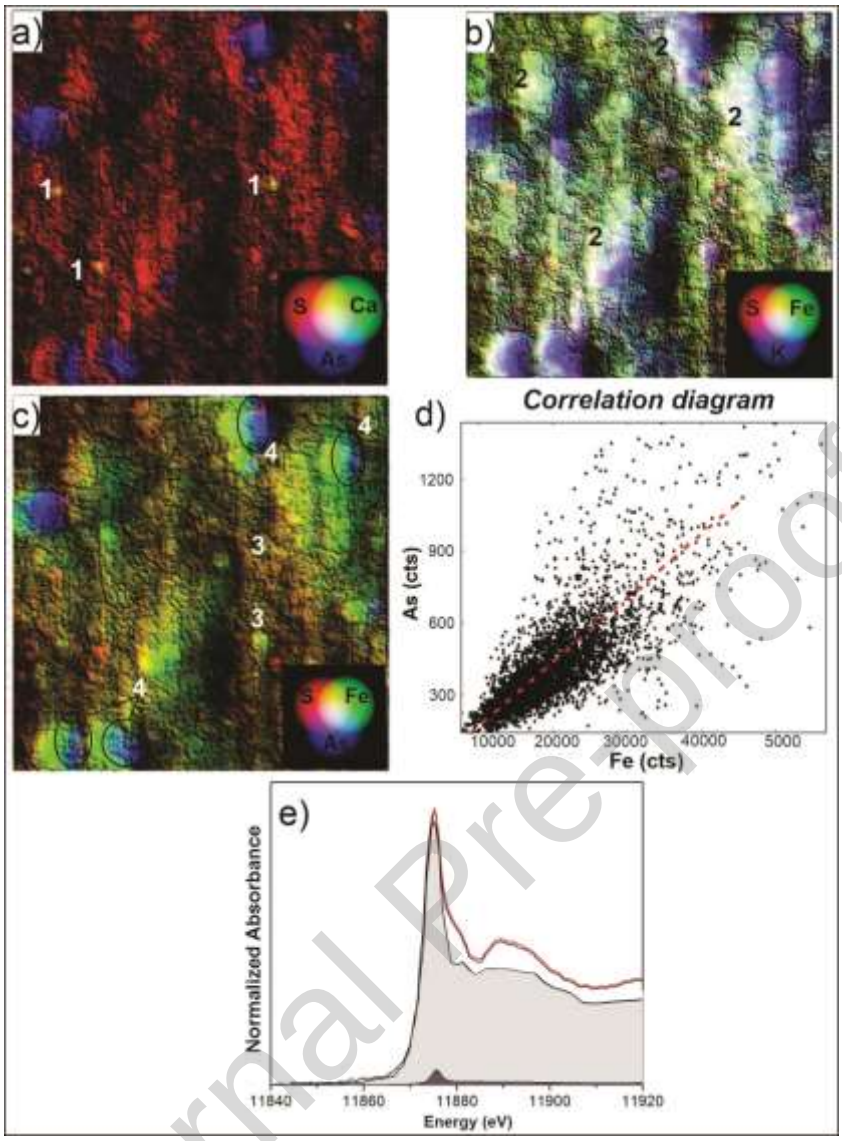

FIGURE 5. Elemental maps showing the distribution of a) Ca, As and S; b) Fe, S, and As in individual grains of the sample collected from the Concordia streambed during the dry season; c) dispersion diagram showing the strong correlation between As and S in the sample; d) results of linear combination fits performed on As K-edge μXANES data collected from As-rich areas of individual grains.

μ-XRF maps performed in samples of the salts accumulated at the streambed and riverbanks during the dry season, show that As is more homogeneously distributed, and clearly associated with Fe. Like in the case of the salts precipitated on the tailing ‘s walls during the dry season, elemental associations also indicate the presence of As-free gypsum (Fig. 6a, spot 1). On the other hand, the frequently observed Fe – S rich particles that correspond to the poorly crystalline schwertmannite, also contain As (Fig. 6b, spot 2). Like in the previous case, LCF analysis of the As K-

Journal Pre-proof

edge μ-XANES spectra obtained from the As rich zones (Fig. 6d) also revealed the presence of adsorbed arsenates and Fe arsenates, species that were identified using the spectra of Na_2HAsO_4, and scorodite mineral as standards representing these potential chemical species respectively. Because the analysed As-rich zones are attached to the schwertmannite grains, the LCF results are interpreted to correspond to arsenate ions adsorbed onto this mineral, while $FeASO_4$ is considered to correspond to thin amorphous coatings precipitated at the surface.

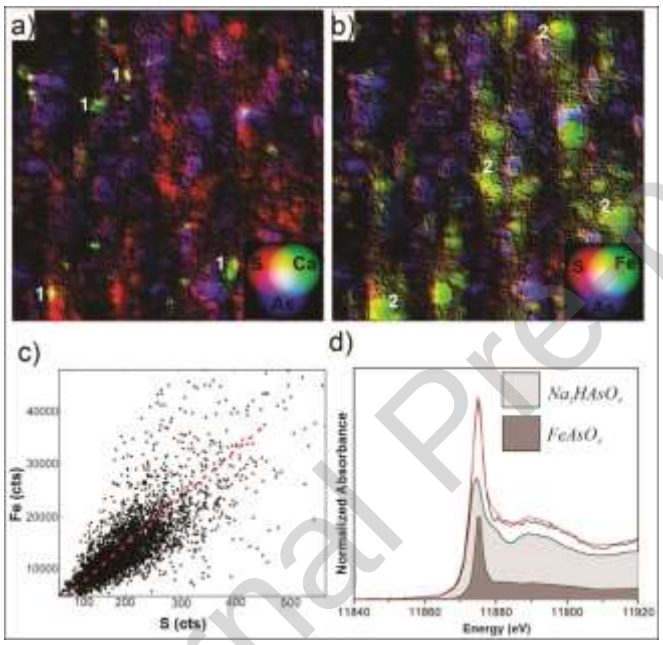

FIGURE 6. Elemental maps showing the distribution of a) Ca, As and S; b) Fe, S, and K, and c) Fe, S, and As in individual grains of the sample collected from the tailings 'walls during the dry season; d) dispersion diagram showing the strong correlation between As and Fe in the sample; e) results of linear combination fits performed on As K-edge μXANES data collected from As-rich areas of individual grains.

5. Factors that control the mineralogy of the evaporitic phases in the mine site

As reported in many sulfide mine sites worldwide (i.e., Frau, 2000; Jerz and Rimstidt, 2003; Hammarstrom et al., 2005; Velasco et al., 2005; Stumbea et al., 2019), the chemical and mineralogical variability of the efflorescent sulfates precipitated on the Concordia streambed and tailing´s sidewalls under contrasting hydrological conditions are controlled by the wetting-drying seasonal cycles of the region. In the study area, wetting consists of occasional, short rainfall events, which mainly occur during the

austral summer months. Consequently, the site is never flooded, and the oscillation of the redox conditions never occurs in either the wastes or the riverbed sediments. Instead, over the past 30 years, a progressive oxidation of the metal sulfides accumulated in the tailing dams has occurred (i.e., Nieva et al., 2019). This is evident not only from the chemical and mineralogical composition of the tailing dams 'wastes but also in the mineral assemblages of the study salts, which are composed exclusively of the oxidized species of the redox-sensitive elements (i.e. metal sulfates, ferric oxyhydroxy-sulfates, and arsenates). The absence of transient reducing conditions has also implications on the release of metal(oids) to the water in contact with these salts, as it prevents the reductive dissolution of the Fe (hydr)oxides and the concurrent release of the adsorbed elements, particularly As. This a common process in farm soils, wetlands and coastal soils affected by periodic waterlogged conditions (e.g., Garcia et al., 2007; Frohne et al., 2011; Fan et al., 2014; Shaheen et al., 2016; LeMonte et al., 2017). In addition to climatic conditions, the mineralogy of the salts also depends on their location in the landscape of the mine site, because this factor controls the extent of exposure of the salts to the atmospheric conditions.

Unlike the efflorescent salts formed in more sheltered areas, such as tailing's sidewalls or within the wastes, that mostly consist of Fe sulfates, the crystalline salts precipitated on the Concordia streambed and riverbanks mainly correspond to assemblages of hydrated Mn, Mg, and Fe sulfates, whose proportions vary along the hydrological year. During the dry season, the mineral assemblage that dominates the thin saline crust deposited on the Concordia riverbanks consists of apjohnite + quartz + epsomite + halotrichite, while at the end of the wet season, the main mineral assemblage in the whitish efflorescent salts consists of epsomite + tamarugite + szmikite + goslarite. Because all these hydrated sulfates are highly soluble, they generally crystallize in open areas exposed to intense evaporation in arid climates (Marszałek et al., 2020). Minerals of the halotrichite group such as apjohnite ($Mn^{2+}Al_2(SO_4)_4 \cdot 22H_2O$) and halotrichite ($Fe^{2+}Al_2(SO_4)_4 \cdot 22H_2O$), are more stable and

precipitate later than the simple magnesium sulfates such as epsomite (e.g. Jerz and Rimstidt, 2003; Hammastron et al., 2005). In the study area, aluminium is provided by the alteration by acidic waters, of feldspars, micas, clays or other aluminosilicates present in the regional rocks and transported downflow by the runoff. At the mine site, runoff waters mix with the metal/sulfate-rich acid mine drainage and, after prolonged periods of evaporation, Al usually precipitates in the form of sulfates of the halotrichite group. On the other hand, the Mg/Na/Mn/Zn hydrated sulfates that compose the salts collected at the end of the wet season, are likely products of the early stages of evaporation of the stream acid waters, as it was observed in similar environments worldwide (e.g., Jambor et al. 2000; Valente and Gomes, 2009; Farkas et al., 2009; Stumbea et al., 2019). Previous experimental results showed preferential precipitation of Mg over Fe sulfate salts from metal-rich mine waters at evaporation rates lower than 70% (Chou and Seal, 2003; Basallote et al., 2019), which might be a likely condition in the Concordia´s riverbanks during the more humid season. Goslarite formation is the product of the direct evaporation of Zn^{2+} and SO_4^{2-} rich solutions that are released during the sphalerite oxidation (Buzatu et al., 2015), one of the main mineral ores in the Concordia Mine (Nieva et al. 2016). In addition to these soluble salts formed by evaporation of metal-rich acid waters, some other minerals are also present in the saline crusts accumulated on the streambed and riverbanks. For example, jarosite is a direct product of the oxidation of pyrite and because it is nearly insoluble, it can be transported in suspension by runoff water from the tailings where this mineral form (i.e., Nieva et al., 2019) to the riverbanks where it accumulates. About 60-65 % of the Fe present in the riverbank salts is in the form of jarosite, while 30-33 % is present in the form of schwertmannite, a poorly crystalline mineral identified by LCF of the XANES spectra.

The soluble fraction of the salts precipitated on the tailing's sidewalls during the dry season represents only 30% of their total mass, due to the presence of quartz and

muscovite as major minerals. Therefore, the mineral assemblage composed of the hydrated and the hydroxy-sulfates gypsum + jarosite + As-jarosite + szmikite must account for the chemical composition of the soluble fraction, characterized by relative much higher contents of Fe than those of Mg and Mn. Surprisingly, the only crystalline phases that could contribute Fe to the solution are jarosite and As-jarosite, two minerals that are relatively insoluble. Thus, the contents of Fe measured in the sample leachate must result from the dissolution of a soluble and poorly crystalline Fe-bearing salt, likely schwertmannite. This mineral, identified by LCF of the Fe-XANES spectra, bears more than 30% of the bulk Fe in the sample. The values available in the literature of the solubility product of this ferric oxyhydroxy-sulfate mineral are variable, but all of them are relatively high suggesting that this mineral is readily soluble, especially at acidic pH values. Bigham et al. (1996) proposed 10^{18} as the solubility product of schwertmannite, while Yu et al (2002) estimated a log K value of 2.01 ± 0.30 and suggested that the solubility of this mineral may vary depending on the content of sulfate. The dissolution of the amorphous Fe(III) arsenates identified by XANES and by μXRF mapping, may also release Fe to the water, but likely in much lower proportion than schwertmannite as this phase is significantly less soluble, with a solubility product of 10^{-23} (Langmuir, 2006).

At the end of the wet season, copiapite is the main crystalline salt precipitated at the tailing´s sidewalls, with minor presence of jarosite, which is a direct product of the oxidation of pyrite. LCF analysis of the Fe K-edge XANES spectra and the Fe-EXAFS results also suggest the presence of schwertmannite, and an Fe(III) sulfate compound that contains As, which could be assigned to the arsenate bearing Fe(III) sulfates defined by Paktunc et al (2013). Copiapite is a water soluble sulfate that precipitates from acid solutions (pH ~2.0) generated when rainfall that infiltrates in the wastes removes loosely bound compounds, and finally precipitates under relatively

humid conditions (i.e., Relative Humidity = 65%; Jerz and Rimstidt, 2003), generally at the initial stages of evaporation (Basallote et al., 2019).

The presence of the Fe(II)-Fe(III) hydrated sulfates copiapite and coquimbite within the wastes matrix is also consistent with elevated relative humidity, and indicates progressive oxidizing conditions. In these salts, about 33% of the bulk Fe is in the form of amorphous or poorly crystalline schwertmannite, while the proportion associated with jarosite is lower than 5%.

6. As speciation in the evaporitic phases of the mine site

In a previous work, Nieva et al (2016) suggested that the rapid release of As during the interaction between the wastes of the tailing dams and the water is associated with the dissolution of highly soluble sulfates. Lower and slower contributions correspond to desorption from Fe oxy-hydroxides or oxy-hydroxy-sulfates and from the alteration of less soluble phases such as As-jarosite. The current analysis of the salts and efflorescences precipitated in the site, also highlight the role of the mineralogy in the scavenging of As, which in turn is controlled by local and regional factors, such as the extent of exposure to the atmospheric conditions of the place of salt precipitation and the climatic conditions respectively.

The highest concentrations of As were determined in the water soluble salts precipitated during the wet season in the walls and pores of the wastes accumulated in the tailing dams, in sectors that are not directly exposed to rainfall. On the other hand, efflorescences and saline crusts formed at the Concordia streambed and riverbanks show significantly lower capacity to scavenge this element. The solid speciation of As in these salts reveals that this element is present in the form of arsenate, mostly associated with jarosite and schwertmannite, regardless the climatic conditions at the moment of the salt precipitation. The amount of arsenic that may be incorporated into jarosite is low, typically less than 10 wt.% AsO_4 (i.e., Salzsauler et al., 2005; Packtunc and Dutrizac, 2003). On the contrary, schwertmannite is known to be an effective

scavenger of As (Fukushi et al., 2003; Regenspurg and Peiffer, 2005; Burton et al., 2009; Cruz Hernandez et al., 2019) through pH-dependent adsorption (Regenspurg and Peiffer, 2005; Burton et al., 2009; Maillot et al., 2013) or co-precipitation (Park et al., 2016). In the efflorescent salts precipitated at the Concordia´s riverbank, the low concentrations of As are distributed in nearly similar proportions between jarosite and schwertmannite during the dry season. In such salts, μXRF mappings show that the spatial distribution of As is closely associated with that of S, suggesting either adsorption on schwertmannite and/or arsenate by sulfate substitution in jarosite, while a lower proportion is present in the form of arsenate coatings formed at the borders of the Fe sulfate grains. In the wet season, the concentration of As in the salts is even lower than in the dry season, and the solid speciation indicates that this element is mostly associated with schwertmannite.

The low concentration of As determined in the water soluble phases of the efflorescent salts formed at the Concordia riverbanks contrast with the relatively high concentrations of this element in the efflorescent salts formed at the exposed walls and pores of the mine wastes accumulated in the tailing dams, especially during the wet season. In conditions of high relative humidity, the Fe(II)-Fe(III) hydrated sulfates copiapite and coquimbite are the dominant crystalline phases in these salts. Jamieson et al. (2005) measured average As concentrations of 64 mg Kg^{-1} in copiapite samples collected from Richmond mine, and suggested that the storage capacity of potentially hazardous elements, such as As, is relatively modest. However, the concentration of the soluble As measured in the sample collected from the tailing´s sidewalls at the end of the wet season, composed of more than 75% of copiapite, is higher than 750 mg Kg^{-1}, which indicates that the capacity of As storage of this salt is important. The structural arrangement of Fe and As in this sample is similar to the local structure of ferric arsenate-sulfate compounds reported by Paktunc et al (2013), in which arsenate may substitute up to 50 % of the sulfate sites. The identification of structural arsenic in

copiapite has important environmental implications due to the elevated solubility of this salt.

CONCLUSIONS

The intense evaporation that affects the As-rich leachates generated by the oxidative dissolution of sulfide-rich mine wastes accumulated in the abandoned tailing dams of the La Concordia mine, trigger the precipitation of saline crusts and efflorescences at the exposed walls and pores. Besides, the evaporation of the leachates that infiltrate through the wastes and reach lower areas in the mine site also favor the precipitation of salts at the Concordia´s streambed and riverbanks. The mineralogical composition of these salts is variable, depending on the regional climatic conditions (i.e., alternating dry and wet seasons), and also on the extent of exposure to the atmospheric agents of the place in which the salt precipitates. The nature of the newly formed minerals also have strong influence on the distribution of arsenic between the solution and the solid phase.

In highly exposed areas such as the streambed and riverbanks, salts are mostly composed of simple hydrated sulfates or minerals of the halotrichite group, which have a low capacity to scavenge As. Therefore, in this part of the mine site, As mostly remains associated with jarosite and schwertmannite, minerals that are stable along the entire hydrological year, but are just minor constituents of these salts.

During the dry season, the tailing's walls are covered by a relative thick crust of red salts composed of clastic minerals, likely wind-blown particles that are attached to the walls by action of the intense winds, associated with some hydrated sulfates, jarosite, schwertmannite and Fe(III) arsenates. The fraction of soluble As in these salts is high, and it might be mostly accounted by arsenate complexes adsorbed onto schwertmannite, while a lower contribution could be expected from the partial dissolution of amorphous Fe(III) arsenates. In the wet season, copiapite is the dominant mineral in the salts precipitated at the tailing´s sidewalls and also in the

Journal Pre-proof

wastes pores. The spectroscopic evidences revealed that As is present in the form of arsenate substituting sulfate in a structural arrangement that might be assigned to copiapite. The association of As with copiapite may explain the elevated concentrations of this element in the salts formed at the tailing´s sidewalls and pores during the wet season. Thus, copiapite may be considered as one of the most important transient reservoirs of As in the mine site as it can release this hazardous pollutant during the occasional rainfall events produced during the wet season. On the contrary, hydrated sulfates, such as gypsum and epsomite, that are more frequently present in the salts formed at the streambed and riverbanks, show a very low capacity to scavenge As. Therefore, unlike copiapite, the dissolution of these salts during rainfall events does not contribute high concentrations of As to the streamwater.

Acknowledgements

The authors wish to acknowledge the assistance of LNLS (Campinas-Brasil), CONICET (PIP Nº 11220150100484CO), ANPCyT (FONCyT PICT 2015-0313), and SECyT-UNC (SECYT CONSOLIDAR – UNC), for their support and the facilities used in this investigation. L. Borda and N.E. Nieva acknowledges doctoral and postdoctoral fellowships from CONICET. L. Borgnino and M.G. Garcia are members of CICyT in Argentina´s CONICET. We thank the staff of the Laboratorio Nacional de Luz Sincrotron (LNLS), particularly to Drs. Santiago Figueroa and Carlos Perez for their helpful suggestions and technical assistance. Thanks to Andrea Lojo and Cecilia Blanco for their technical assistance during ICP-MS analysis and Rietveld refinement respectively. We are especially grateful to the two anonymous reviewers and the editor for suggesting significant improvements to this manuscript.

Journal Pre-proof

References

Alpers, C.N., Blowes, D.W., Nordstrom, D.K., Jambor, J.L., 1994. Secondary minerals and acid mine-water chemistry. In: Jambor, J.L, Blowes, D.W. (Eds.). Environmental Geochemistry of Sulfide Mine-Wastes. Mineralogical Association of Canada Short Course Vol. 22, 247-270.

Alpers, C.N., Jambor, J.L., Nordstrom, D.K., (Eds.), 2000. Sulfate Minerals – Crystallography, Geochemistry, and Environmental Significance. Reviews in Mineralogy and Geochemistry Vol. 40.

Argañaraz, R., Mancini, J., Sureda, R., 1982. El yacimiento de Concordia (Ag-Pb) en la provincia de Salta, Argentina. Un proyecto de rehabilitación y explotación minera. 5° Congreso Latinoamericano de Geología, Actas 5, 61–78.

Basallote, M.D., Cánovas, C.R., Olías, M., Pérez-López, R., Macías, F., Carrero, S., Ayora, C., Nieto, J.M., 2019. Mineralogically-induced metal partitioning during the evaporative precipitation of efflorescent sulfate salts from acid mine drainage. Chemical Geology

Bayless, E.R., Olyphant, G.A., 1993. Acid generating salts and their relationship to the chemistry of groundwater and storm runoff at an abandoned mine site in southwestern Indiana, USA. J Contam Hydrol 12, 313–328

Bia, G., Garcia, M.G., Borgnino, L., 2017. Changes in the As solid speciation during weathering of volcanic ashes: a XAS study on Patagonian ashes and Chacopampean loess. Geochim. Cosmochim. Acta 212, 119–132.

Bianchi, D., Yanez, A., 1992. Las precipitaciones en el NOA Argentino, Segunda Edición. INTA Salta.

Bigham, J.M., Schwertmann, U., Traina, S.J., Winland, R.L., Woolf, M., 1996. Schwertmannite and the chemical modeling of iron in acid sulfate waters. Geochim. Cosmochim. Acta 60, 2111–2121.

Journal Pre-proof

Bigham, J.M., Nordstrom, D.K., 2000. Iron and aluminum hydroxysulfates fromacid sulfate waters. In: Alpers, C.N., Jambor, J.L., Nordstrom, D.K. (Eds.), Sulfate Minerals Crystallography, Geochemistry, and Environmental Significance. Rev. Mineral. Geochem. 40, 351–403.

Burton, E.D., Watling K.M., Johnston, S.G., Bush, R.T., 2009. Arsenic Effects and Behavior in Association with the Fe(II)-Catalyzed Transformation of Schwertmannite. Environmental Science and Technology 44, 2016-2021 ·

Buzatu, A., Dill H.G., Buzgar, N., Damian, G., Maftei, A.E., Apopei A.J., 2016. Efflorescent sulfates from Baia Spriemining area (Romania) — Acid mine drainage and climatological approach. Science of the Total Environment. 542, 629–641

Cánovas, C.R., Olías, M., Nieto, J.M., Galván, L., 2010. Wash-out processes of evaporitic sulfate salts in the Tinto river: hydrogeochemical evolution and environmental impact. Appl. Geochem. 25 (2), 288–301.

Cánovas, C.R., Riera, J., Carrero, S., Olías, M., 2018. Dissolved and particulate metal fluxes in an AMD-affected stream under different hydrological conditions: The Odiel River (SW Spain). Catena 165, 414-424.

Chou, I.M., Seal II, R.R., 2003. Determination of epsomite–hexahydrite equilibria by the humidity buffer technique at 0.1MPa with implications for phase equilibria in the system MgSO4–H2O. Astrobiology 3, 619– 630.

Cruz-Hernández, P., Carrero, S., Pérez-López, R., Fernández-Martínez, A., Lindsay, M.B.J, De Joie, C., Nieto, J.M., 2019. Influence of As(V) on precipitation and transformation of schwertmannite in acid mine drainage-impacted waters (in press).

Dold, B., 1999. Mineralogical and geochemical changes of copper flotation tailings in relation to their climatic settings and original composition—implications for acid mine drainage and element mobility. PhD thesis, Terre et Environement, vol. 18. 230 pp.,Geneva.

Drahota, P., Filippi, M., 2009. Secondary arsenic minerals in the environment: a review. Environ. Int. 35, 1243–1255.

Drahota. P., Knappová, M., Kindlová, H., Culka, A., Majzlan, J., Mihaljevič, M., Rohovec, J., Veselovský, F., Fridrichová, M., Jehlička, J., 2016. Mobility and attenuation of arsenic in sulfide-rich mining wastes from the Czech Republic. Science of The Total Environment. 558, 192-203.

Fan, J.X., Wang, Y.J., Liu, C., Wang, L.H., Yang, K., Zhou, D.M., 2014. Effect of iron oxide reductive dissolution on the transformation and immobilization of arsenic in soils: new insights from X-ray photoelectron and X-ray absorption spectroscopy. J. Hazard. Mater. 279, 212–219.

Farkas, I. M., Weiszburg, T. G., Pekker, P., Kuzmann, E. 2009. A half-century of environmental mineral formation on a pyrite-bearing waste dump in the mátra mountains, Hungary. Canadian Mineralogist 47, 509-524.

Forsyth J. B., Hedley I. J. and Johnson C. E., 1968. The magnetic structure and hyperfine field of goethite (a-FeOOH). J. Phys. C 1, 179–188.

Frau, F., 2000. The formation–dissolution–precipitation cycle of melanterite at the abandoned pyrite mine of Genna Luas in Sardinia, Italy: environmental implications. Mineralogical Magazine 64, 995-1006.

Frohne, T., Rinklebe, J., Diaz-Bone, R. A., Du Laing, G., 2011. Controlled variation of redox conditions in a floodplain soil: Impact on metal mobilization and biomethylation of arsenic and antimony. Geoderma. 160 (3−4), 414−424Fukushi, K., Sasaki, M., Sato, T., Yanase, N., Amano, H., Ikeda, H., 2003. A natural attenuation of arsenic in drainage from an abandoned arsenic mine dump. Appl Geochem 18, 1267–1278

Gaiero, D.M., Simonella, L., Gassó, S., Gili, S., Stein, A.F., Sosa, P., Becchio, R., Arce, J., Marelli, H., 2013. Ground/satellite observations and atmospheric modeling of dust storms originating in the high Puna-Altiplano deserts (South America):

Implications for the interpretation of paleo-climatic archives. Journal of Geophysical Research Atmospheres, 118 (9), 3817-3831.

Hammarstrom, J.M., Seal II, R.R., Meierb, A.L., Kornfeld, J.M., 2005. Secondary sulfate minerals associated with acid drainage in the eastern US: recycling of metals and acidity in surficial environments. Chemical Geology 215, 407– 431.

Jambor, J.L., Nordstrom, D.K. Alpers, C.N., 2000. Metal–sulfate salts from sulfide mineral oxidation. In Sulfate Minerals – Crystallography, Geochemistry and Environmental Significance (C.N. Alpers, J.L. Jambor & D.K. Nordstrom, eds.). Rev. Mineral. Geochem. 40, 303-350

Jamieson, H., Robinson, C., Alpers, C.N., McCleskey, R.B., Nordstrom, D.K., Peterson, R.C., 2005. Major and trace element composition of copiapite-group minerals and coexisting water from the Richmond mine, Iron Mountain, California. Chem. Geol. 215, 387–405.

Jerz, J.K., Rimstidt, J.D., 2003. Efflorescent sulfate minerals: paragenesis, relative stability and environmental impact. Am. Mineral. 88, 1919–1932

Kitahama, K., Kiriyama, R., Baba, Y., 1975. Refinement of the crystal structure of scorodite. Acta Crystallogr. B 31, 322–324.

Kocourková, E., Sracek, O., Houzar, S., Cempírek, J., Losos, Z., Filip, J., Hršelová, P., 2011. Geochemical and mineralogical control on the mobility of arsenic in a waste rock pile at Dlouhá Ves, Czech Republic. Journal of Geochemical Exploration 110, 61–73.

Langmuir, D., Mahoney, J., MacDonald, A., Rowson, J., 2006. Solubility products of amorphous ferric arsenate and crystalline scorodite (FeAsO42H2O) and their application to arsenic behavior in buried mine tailings. Geochim. Cosmochim. Acta 70 (12), 2942–2956.

LeMonte, J. J., Stuckey, J. W., Sanchez, J. Z., Tappero, R., Rinklebe, J., Sparks, D.L., 2017. Sea level rise induced arsenic release from historically contaminated coastal soils. Environ. Sci. Technol., 2017, 51 (11), 5913–5922.

Lottermoser, B.G., Ashley, P.M., 2006. Physical dispersion of radioactive mine waste at the rehabilitated Radium Hill uranium mine site, South Australia. Aust. J. Earth Sci. 53, 485–499.

Lottermoser, B.G., 2010. Mine Wastes: Characterization, Treatment and Environmental Impacts. third ed. Springer, Berlin, Heidelberg, p. 400.

Maillot, F.,Morin, G., Juillot, F., Bruneel, O., Casiot, C., Ona-Nguema, G.,Wang, Y., Lebrun, S., Aubry, E., Vlaic, G., Brown Jr., G.E., 2013. Structure and reactivity of As(III)- and As(V)- rich schwertmannites and amorphous ferric arsenate sulfate from the Carnoules acid mine drainage, France: comparison with biotic and abiotic model compounds and implications for As remediation. Geochim. Cosmochim. Acta 104, 310–329.

Majzlan, J., Plášil, J., Škoda, R., Gescher, J., Kögler, F., Rusznyak, A., Küsel, K., Neu, T.R., Mangold, S., Rothe, J., 2014. Arsenic-Rich Acid Mine Water with Extreme Arsenic Concentration: Mineralogy, Geochemistry, Microbiology, and Environmental Implications. Environ Sci Technol. 48, 13685-13693

Marszałek, M., Gaweł, A., Włodek, A., 2020. Pickeringite from the Stone Town Nature Reserve in Ciężkowice (the Outer Carpathians, Poland). Minerals 10, 187.

Menchetti S. and Sabelli C., 1976. Crystal chemistry of the alunite series: crystal structure refinement of alunite and synthetic jarosite. NeuesJahrb. Mineral., Geol. Palaontol., Monatsh, 406– 417.

Nieva, N.E., Borgnino, L., Locati, F., García, M.G., 2016. Mineralogical control on arsenic release during sediment–water interaction in abandoned mine wastes from the Argentina Puna. Sci. Total Environ. 550, 1141–1151.

Nieva, N.E., Borgnino, L., García, M.G., 2018. Long term metal release and acid generation in abandoned mine wastes containing metal-sulphides. Environ. Pollut. 242, 264–276.

Journal Pre-proof

Nieva, N.E., Bia, G., García, M.G., Borgnino, L., 2019. Synchrotron XAS study on the As transformations during the weathering of sulfide-rich mine wastes. Sci. Total Environ. 669, 798–811.

Nordstrom, D.K., Alpers, C.N., 1999. Geochemistry of acid mine waste. In: Plumlee, G.S., Londgson, M.J. (Eds.), The Environmental Geochemistry of Ore Deposits. Part A: Processes, Techniques, and Health Issues. Reviews in Economic Geology, pp. 133–160.

O'Day, P.A., Rivera, N., Root, R., Carroll, S.A., 2004. X-ray absorption spectroscopic study of Fe reference compounds for the analysis of natural sediments. Am. Mineral. 89, 572–585.

Olyphant, G.A., Bayless, G.R., Harper, D., 1991. Seasonal and weather-related controls on solute concentrations and acid drainage from a pyritic coal-refuse deposit in southwestern Indiana, USA. J. Contam. Hydrol. 7, 219–236.

Paktunc, D., Dutrizac, J.E., 2003. Characterization of arsenic substitution in synthetic potassium jarosite using X-ray diffraction and X-ray absorption spectroscopy. Canadian Mineralogist. 41, 905–919

Park, J.H., Han, J., Ahn, J.S., 2016. Comparison of arsenic co-precipitation and adsorption by iron minerals and the mechanism of arsenic natural attenuation in a mine stream. Water Research. 106, 295-303

Paktunc, D., Majzlan, J., Palatinus, L., Dutrizac, J., Klementová, M., Poirier, G., 2013. Characterization of ferric arsenate-sulfate compounds: Implications for arsenic control in refractory gold processing residues. American Mineralogist. 98, 554–565.

Pérez, C.A., Radtke, M., Sanchez, H.J., Tolentino, H., Neuenshwander, R.T., Barg, W., Rubio, M., Bueno, M.I.S., Raimundo, I.M., Rohwedder, J.J.R., 1999. Synchrotron radiation X-ray fluorescence at the LNLS: beamline instrumentation and experiments, X-Ray Spectrom. 28, 320–326.

Journal Pre-proof

Regenspurg, S., Pfeiffer, S., 2005. Arsenate and chromate incorporation in schwertmannite. Appl Geochem 20, 1226–1239

Rietveld, H.M., 1969. A Profile refinement method for nuclear and magnetic structures, J. Appl. Crystallogr. 2, 65–71.

Rodríguez-Carvajal, J., 1993. Recent advances in magnetic structure determination by neutron powder diffraction, Physica. 192, 55–69.

Salzsauler, K.A., Sidenko, N.V., Sherriff, B.L., 2005. Arsenic mobility in alteration products of sulfide-rich, arsenopyrite-beairng mine wastes, Snow Lake, Manitoba, Canada. Appl Geochem 20, 2303–2314

Savage, K.S., Bird, D.K., O'Day, P.A., 2005. Arsenic speciation in synthetic jarosite. Chem. Geol. 215, 473–498.

Shaheen, S.M., Rinklebe, J., Frohne, T., White, J.R., DeLaune, R.D., 2016. Redox effects release kinetics of arsenic, cadmium, cobalt, and vanadium in Wax Lake Deltaic freshwater marsh soils. Chemosphere 150, 740−748.Stumbea, D., Chicoș, M.M., Nica, V., 2019. Effects of waste deposit geometry on the mineralogical and geochemical composition of mine tailings. Journal of Hazardous Materials 368.

Valente, T.M., Gomes, C.L., 2009. Occurrence, properties and pollution potential of environmental minerals in acid mine drainage, Sci. Total Environ. 407, 1135–1152.

Velasco, F., Alvaro, A., Suarez, S., Herrero, J.M., Yusta, I., 2005. Mapping Fe-bearing hydrated sulphate minerals with short wave infrared (SWIR) spectral analysis at San Miguel mine environment, Iberian Pyrite Belt (SW Spain). Journal of Geochemical Exploration. 87, 45-72

Waychunas, G.A., Xu, N., Fuller, C.C., Davis, J.A., Bigham, J.M., 1995. XAS study of AsO_4^{3-} and SeO_4^{2-} substituted schwertmannites. Physica B 208 and 209, 481–483.

Yu, J., Park, M., Kim, J., 2002. Solubilities of synthetic schwertmannite and ferrihydrite Geochemical Journal. 36, 119-132.

Zappettini, E.O., 1990. Mineralizaciones polimetálicas de los distritos El Queva, La Poma- Incacchule y Concordia, Salta. In: Zappettini, E.O. (Ed.), Recursos minerales de la República Argentina Anales 35. Instituto de Geología y Recursos Minerales (SEGEMAR), pp. 1603–1611.

FIGURE CAPTIONS

FIGURE 1. Map of La Concordia mine site showing the location of the sampling points. The images show the characteristics of the salts crusts formed at the Concordia´s streambed and at the tailing sidewalls ans pores in the two sampling periods.

FIGURE 2. Ternary diagram showing the relative contents of Fe, Mn and Mg in the study salt samples.

FIGURE 3. Linear combination fits of the Fe K-edge spectra for the study samples. Thick solid lines depict measured spectra; red solid lines indicate fit results. The quantitative data for the fittings are provided in Table 3. All the reference compounds mentioned in the SI file have been considered in the LCF analysis.

FIGURE 4 Linear combination fits of the As K-edge spectra for the study samples. Thick solid lines depict measured spectra; red solid lines indicate fit results. The quantitative data for the fittings are provided in Table 5. All the reference compounds mentioned in the SI file have been considered in the LCF analysis.

FIGURE 5. Elemental maps showing the distribution of a) Ca, As and S; b) Fe, S, and As in individual grains of the sample collected from the Concordia streambed during the dry season; c) dispersion diagram showing the strong correlation between As and

S in the sample; d) results of linear combination fits performed on As K-edge μXANES data collected from As-rich areas of individual grains.

FIGURE 6. Elemental maps showing the distribution of a) Ca, As and S; b) Fe, S, and K, and c) Fe, S, and As in individual grains of the sample collected from the tailings 'walls during the dry season; d) dispersion diagram showing the strong correlation between As and Fe in the sample; e) results of linear combination fits performed on As K-edge μXANES data collected from As-rich areas of individual grains.

TABLE CAPTIONS

TABLE 1. Mineralogical composition of efflorescent salts from La Concordia Mine

TABLE 2. Chemical composition the water-soluble fraction of the study samples after 24 h of salt-water reaction.

TABLE 3. Results of linear combination fits of the Fe K-edge XANES spectra of the Concordia mine salt samples collected during the dry and wet seasons. The energy range in the normalized XANES spectra was 7100–7220 eV. Values in parenthesis correspond to the standard deviation. The residual factor (R) and χ^2 provide a measure of the goodness of the fit.

TABLE 4. EXAFS fitting results at the Fe K-edge for the sample TW-D and TW-W. Experimental and calculated curves are shown in the SI file. Fitted parameters include: N, coordination number, R (Å), interatomic distance, σ2 (Å2), squared Debye-Waller factor, ΔE0 (eV), energy difference accounting for phase shift between overall experimental spectrum and FEFF calculation.

TABLE 5 Results of linear combination fits performed on As K-edge XANES data of the salt samples. Linear combinations were performed with the software Athenas (Ravel and Newville, 2005). The energy range in the normalized XANES spectra was

Journal Pre-proof

11,840–11,920 eV. The residual factor (R) and χ^2 provide a measure of the goodness of the fit.

TABLE 6. EXAFS fitting results at the As K-edge of the studied samples. Experimental and calculated curves are shown in the SI file. Fitted parameters include: N, coordination number, R (Å), interatomic distance, σ2 (Å2), squared Debye-Waller factor and ΔE0 (eV), energy difference accounting for phase shift between overall experimental spectrum and FEFF calculation.

Graphical abstract

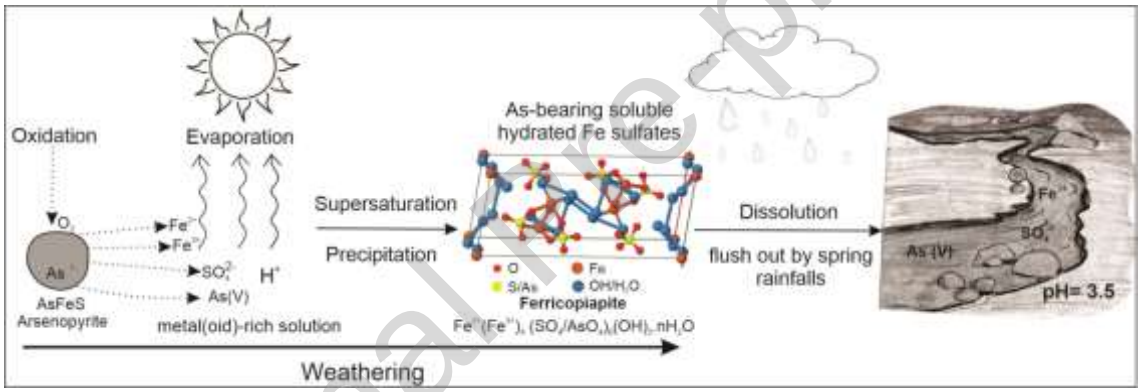

Journal Pre-proof

CRediT author statement

N. E. Nieva: Conceptualization, Formal analysis, Investigation, Visualization, Writing - Original Draft; **M. G. Garcia**: Conceptualization, Investigation, Writing - Review & Editing, Supervision, Project administration, Funding acquisition; **L. Borgnino:** Conceptualization, Investigation, Writing-Original Draft, Supervision, Funding acquisition; **L. G. Borda:** Formal analysis

Journal Pre-proof

Declaration of interests

☒ The authors declare that they have no known competing financial interests or personal relationships that could have appeared to influence the work reported in this paper.

☐The authors declare the following financial interests/personal relationships which may be considered as potential competing interests:

Journal Pre-proof

Highlights

- The evaporation of AMD triggers the precipitation of saline crusts at the Concordia mine site
- The newly formed minerals have strong influence on the distribution of arsenic between the solution and the solid phase.
- The highest concentrations of As in the mine site are associated with copiapite
- As is present in the form of arsenate substituting sulfate in copiapite
- Gypsum and epsomite show a very low capacity to scavenge As

Journal Pre-proof